Published in "Nature doi:10.1038/nature10649, 2011"
which should be cited to refer to this work.

The circadian molecular clock creates epidermal stem cell heterogeneity

Peggy Janich[1], Gloria Pascual[1], Anna Merlos-Suárez[2], Eduard Batlle[2,3], Jürgen Ripperger[4], Urs Albrecht[4], Karl Obrietan[5], Luciano Di Croce[1,3] & Salvador Aznar Benitah[1,3]

Murine epidermal stem cells undergo alternate cycles of dormancy and activation, fuelling tissue renewal. However, only a subset of stem cells becomes active during each round of morphogenesis, indicating that stem cells coexist in heterogeneous responsive states. Using a circadian-clock reporter-mouse model, here we show that the dormant hair-follicle stem cell niche contains coexisting populations of cells at opposite phases of the clock, which are differentially predisposed to respond to homeostatic cues. The core clock protein Bmal1 modulates the expression of stem cell regulatory genes in an oscillatory manner, to create populations that are either predisposed, or less prone, to activation. Disrupting this clock equilibrium, through deletion of *Bmal1* (also known as *Arntl*) or *Per1/2*, resulted in a progressive accumulation or depletion of dormant stem cells, respectively. Stem cell arrhythmia also led to premature epidermal ageing, and a reduction in the development of squamous tumours. Our results indicate that the circadian clock fine-tunes the temporal behaviour of epidermal stem cells, and that its perturbation affects homeostasis and the predisposition to tumorigenesis.

Epidermal stem cells ensure that skin homeostasis is maintained. Murine epidermal stem cells are located either at the permanent portion of the hair follicle—termed the bulge—and are exclusively responsible for hair cycling[1–4]; or at the junction between the epidermis and the hair follicle (isthmus), and feed into the epidermis and sebaceous glands[5–7]. In addition, a continuous proliferation of basal interfollicular epidermal cells ensures daily epidermal maintenance[8].

Bulge stem cells undergo bouts of activation followed by periods of dormancy, to establish hair follicle cycling. Robust TGF-β and Bmp signals act as 'activation breaks', rendering bulge cells dormant during the resting phase of the hair cycle (telogen)[9–11]. At the onset of the growth phase (anagen), bulge cells respond to Wnt signals by migrating into the lower proliferative hair germ region, where they contribute to follicle growth[12–15]. Subsequently, at mid-anagen, the bulge undergoes a second round of activation, which replenishes cells lost at the onset of anagen[2,3]. However, the response of bulge stem cells to activating stimuli is a heterogeneous process, as only a subset of them become active during either stage of activation[12,13]. The nature of such niche heterogeneity is currently unknown. Importantly, perturbing the equilibrium between the responsive and non-responsive stem cell states causes tissue malfunction and increases the risk of carcinogenesis[16–20].

Here, we analysed the role of the molecular clock in fine-tuning the function of epidermal stem cells. The mammalian clock machinery anticipates and synchronizes vital functions related to the physiological circadian needs of the organism[21]. The core molecular clock is established by a positive limb, composed of heterodimers of the transcription factors Clock and Bmal, which drives the rhythmic expression of the negative limb proteins, period (Per1–3), cryptochrome (Cry1/2), and Dec1/2 (ref. 21). Accumulated Per and Cry proteins in turn translocate to the nucleus and inhibit Bmal/Clock transcriptional activity, thereby repressing their own expression and marking the beginning of a new cycle.

Circadian heterogeneity in hair-follicle stem cells

We monitored the activity of the clock in epidermal stem cells by means of a reporter bacterial artificial chromosome (BAC) transgenic mouse, in which the expression of fluorescent venus is under the regulation of the full-length promoter of the *Per1* gene[22]. Venus expression mirrors the endogenous oscillation of the clock in the suprachiasmatic nuclei, where the central pacemaker resides, thereby establishing its bona fide circadian reporter activity[22]. We first studied the behaviour of the clock in the dorsal skin of Per1–venus mice collected between postnatal days (P)19 and P31, when hair follicles synchronously transit from the dormant to the growth phase.

At P19, a stage in which the bulge is predominantly dormant, the bulge cells expressing CD34 and the highest levels of α6 integrin (α6 integrin^{bright}/CD34^{+}) contained a continuum of venus-expressing populations, which could be subdivided into cells with highest mean fluorescence intensity of venus (venus^{bright}), and those with no venus fluorescence (venus^{dim}), as determined by immunohistochemistry (Supplementary Fig. 1), and fluorescence-activated cell sorting (FACS) (Fig. 1a, b). At this stage, the bulge contained approximately equal numbers of venus^{bright} and venus^{dim} stem cells (Fig. 1a, b). As hair follicles synchronously progressed into anagen (from P20 to P31), the proportion of venus^{bright} bulge cells steadily increased, reaching a proportion of 90% venus^{bright} to 10% venus^{dim} at the peak of follicle growth (Fig. 1a, b). Conversely, the basal layer of the interfollicular epidermis (α6 integrin^{bright}/CD34^{-}) showed a homogenous pattern of clock activity with a ratio of 95:5 venus^{bright}:venus^{dim} cells, irrespective of the day analysed (Supplementary Fig. 2). Heterogeneity of the clock phase in bulge cells during the telogen to anagen transition was also observed with another independently generated reporter line, Per1–GFP, as shown by three-dimensional whole-mount GFP fluorescence imaging of tail epidermis (Supplementary Fig. 3a, b)[23].

We next verified whether these clock stem cells states showed circadian rhythmicity. FACS analysis indicated that the expression of venus in bulge stem cells in anagen (P27), or interfolllicular epidermis basal cells, followed a circadian pattern, irrespective of whether the mice were maintained in 12 h light/dark cycles, or in constant darkness under free running conditions (Fig. 1c and Supplementary Fig. 4a, b)[21]. This circadian variation was further confirmed

[1]Center for Genomic Regulation and UPF, 08003 Barcelona, Spain. [2]Institute for Research in Biomedicine, 08028 Barcelona, Spain. [3]Institució Catalana de Recerca i Estudis Avançats (ICREA), 08010 Barcelona, Spain. [4]University of Fribourg, 1700 Fribourg, Switzerland. [5]Ohio State University, Columbus, Ohio 43210, USA.

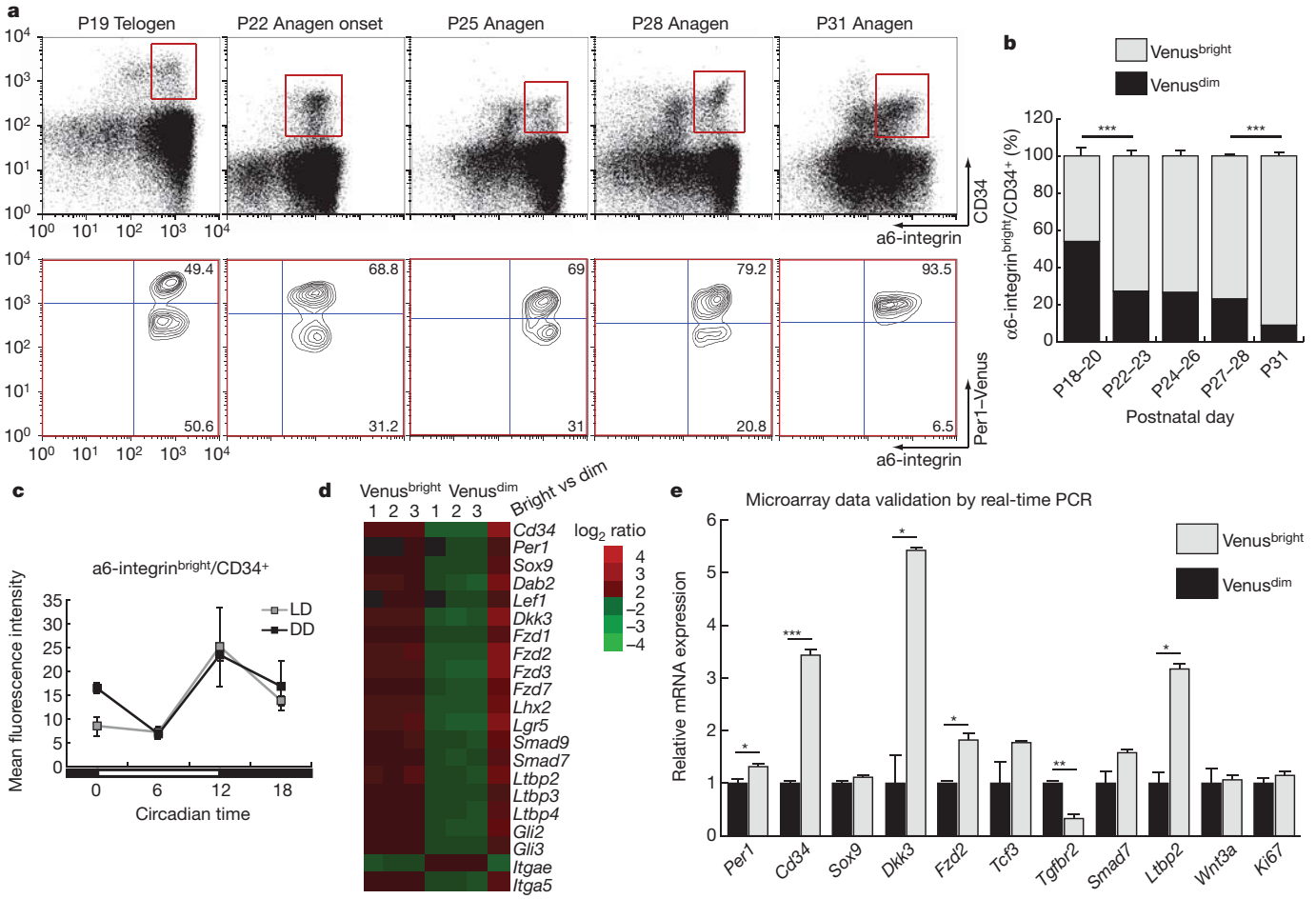

Figure 1 | The molecular clock regulates the expression of the bulge stem cell signature. **a**, **b**, Percentages of venus^{bright} and venus^{dim} cells in the bulge by FACS ($n \geq 6$). **c**, Venus mean fluorescence intensity of bulge cells in mice kept under 12 h light/12 h dark (LD) and 12 h dark/12 h dark (DD) conditions ($n = 2$). **d**, Heatmap of selected genes from arrays of venus^{bright} and venus^{dim} bulge cells of P19 mice ($n = 3$). **e**, Validation of microarray data by real-time PCR. Fold change is shown as relative to venus^{dim} cells after normalization to pumilio 1 (*Pum1*) ($n = 2$, pool of 6 mice per replicate). Results in **b**, **c** and **e** are shown as mean ± s.e.m., $^{*}P < 0.05$, $^{**}P < 0.01$, $^{***}P < 0.001$ (two-tailed Student's *t*-test).

by time-lapse *in vivo* confocal microscopy of venus fluorescence in dorsal skin explants biopsied from adult Per1–venus mice, and GFP fluorescence in whole mounts of tail epidermis of Per1–GFP mice (Supplementary Fig. 4c, d).

The clock regulates stem cell genes

We then compared the global transcriptomes of purified venus^{bright} and venus^{dim} bulge cells from the dorsal skin of P18–19 mice (α6^{bright}/CD34^{+}/venus^{bright} and α6^{bright}/CD34^{+}/venus^{dim}). As expected, both populations showed differential expression of core circadian transcripts, such as *Cry2*, *Per1*, *Nr1d1*, *Rorβ*, *Dec2* and *E4BP4* (also known as *Nfil3*) (Fig. 1d and Supplementary Table 1). Intriguingly, although the bulge is inactive at P18–19, both populations differed in the expression of a significant number of genes previously shown to constitute the bulge signature[2,3,12,24]. Venus^{bright} bulge stem cells expressed higher levels (between 1.4- to 3-fold) of Wnt-signalling factors, including *Tcf3*, *Fzd2/3*, *Sox9*, *Lhx2*, *Lgr5*, *Lef1*, *Dkk3* and *Dab2*, as well as TGF-β-inhibitory factors such as *Smad7*, *Ltbp2–4*, *Smurf*, *Lefty* and *Cul1* (Fig. 1d, e, and Supplementary Table 1). Other pathways differentially expressed relevant for bulge behaviour related to integrins, Notch, Bmp and Shh, among others (Fig. 1d, e).

Thus, the coexisting clock states of dormant bulge stem cells correlated with differential expression of key epidermal homeostasis genes. Promoter analysis revealed that several of these genes, encoding for proteins known to control bulge dormancy, activation, differentiation and niche interactions[1], contained several putative Bmal1/Clock-binding sites within their proximal and distal promoter regions (Supplementary Table 2). These included the Wnt signalling factors *Dab2*, *Lef1*, *Dkk3*, *Fzd2*, *Sox9*, *Lhx2* and *Tcf4*; TGF-β regulators such as *Smad7*, *Lefty*, *Smurf2* and *Smad9*; and *Itga6* as well as modulators of Bmp and Notch signalling (Supplementary Table 2). We confirmed by chromatin immunoprecipitation (ChIP) that Bmal1/Clock bound to these promoters in intact adult tail epidermis (Supplementary Fig. 5a), and that the binding of Bmal1 was circadian (Fig. 2). Chromatin occupancy of Bmal1 to these genes was also confirmed in FACS-sorted bulge stem cells (Supplementary Fig. 5b).

Clock arrhythmia affects homeostasis

We next sought to study the biological significance of this clock mechanism in epidermal stem cells *in vivo*. To this end, we generated mice with a conditional deletion of *Bmal1* in the keratin-14^{+} basal keratinocyte compartment (K14Cre/Bmal1$^{LoxP/LoxP}$, hereafter refered as Bmal1KO) (Supplementary Fig. 6a, b). Deletion of *Bmal1* causes circadian arrhythmicity without the need to perturb any other core circadian member[21], and its ubiquitous deletion causes premature ageing, including defects in adult skin morphogenesis[25–27]. We crossed Bmal1KO and Per1–venus mice, and verified that the circadian clock of bulge stem cells and basal interfollicular epidermal cells was arrhythmic, and permanently skewed towards a clock^{low} (venus^{dim}) state (Supplementary Fig. 6c).

Bulge stem cells and primary keratinocytes isolated from the dorsal skin of Bmal1KO mice expressed lower transcript levels of Wnt-related

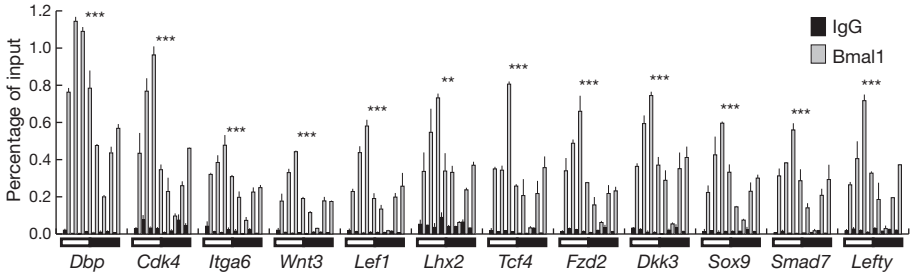

Figure 2 | Circadian binding of Bmal to the promoters of genes involved in adhesion, cell cycle, TGF-β and Wnt pathways. ChIP from tail epidermis of wild-type mice collected every 3 h during 24 h (white and black bars represent day and night, respectively). Graph shows percentage of immunoprecipitated DNA over an input control from one representative experiment ($n = 2$). Results are shown as mean ± s.e.m., $^{**}P < 0.01$, $^{***}P < 0.001$ (one-way ANOVA). Statistical significance determined by Cosinor analysis revealed a P value of $P < 0.05$ for *Dbp* and *Cdk4*, and $P < 0.001$ for *Itga6*, *Lef1*, *Smad7*, *Sox9* and *Tcf4*.

genes including *Dab2*, *Dkk3*, *Lef1* and *Wnt10a*, than control stem cells (Fig. 3a and Supplementary Fig. 5c). In addition, they contained lower messenger RNA levels of TGF-β inhibitors, and higher amounts of *Tgfbr2* and *Smad3* (Fig. 3a and Supplementary Fig. 5c). The expression of Wnt and TGF-β-related factors in purified bulge stem cells varied within a 12 h period in wild-type mice, but not Bmal1KO mice (Supplementary Fig. 5d). Accordingly, the hair follicles of Bmal1KO mice showed the same differences at the protein level, as exemplified by immunohistochemical analysis of Sox9, Lef1, phospho-Smad2 and TGFβR2 in dorsal skin sections, and western blot from primary keratinocytes (Fig. 3b, d).

Altogether, these results indicated that the clock machinery might endow subpopulations of epidermal stem cells with different predispositions to respond to dormancy or activation stimuli, such as TGF-β and Wnt. In line with this, the hair follicle bulge and interfollicular epidermis of Bmal1KO mice contained higher levels of active phospho-Smad2 (Fig. 3b, d). Moreover, Bmal1KO keratinocytes were more responsive to TGF-β treatment than control keratinocytes (Fig. 3c). We could not detect any Wnt activity using the Wnt-specific reporter containing binding sites for TCF/Lef proteins (TOP-Flash) in our primary cultures of mouse keratinocytes stimulated with the GSK3b inhibitor 6-bromoindirubin-3-oxime (BIO), or purified Wnt3a, in accordance with previous reports[28]; this prevented us from further studying the effect of Bmal1 deletion on Wnt responsiveness (Supplementary Fig. 7).

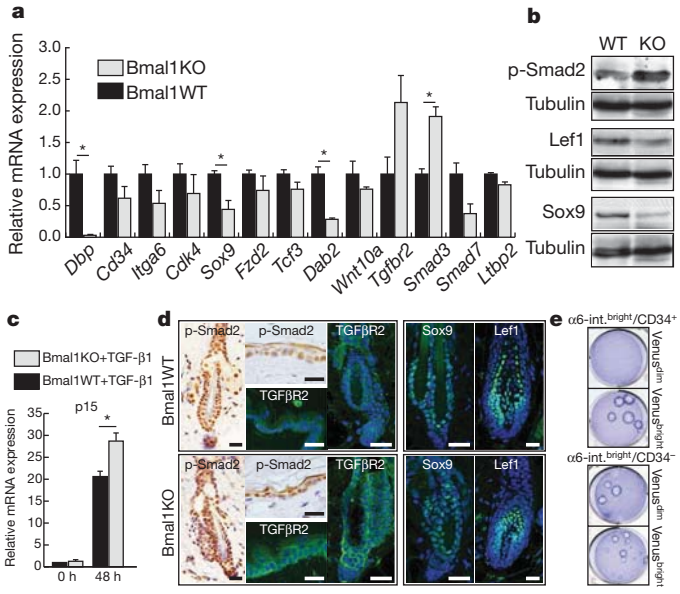

Figure 3 | Bmal1 modulates the response of bulge stem cells to activation and dormancy cues. **a**, Differential expression of genes in bulge cells of Bmal1WT and Bmal1KO mice. Fold-change values are shown as relative expression to Bmal1WT cells after normalization to *Pum1* ($n = 2$). **b**, Western blot analysis for phospho-Smad2 (p-Smad2), Lef1 and Sox9 in tail epidermis of 9-month-old Bmal1WT and Bmal1KO mice; $n = 3$ mice were analysed for each group; **c**, Primary mouse keratinocytes of Bmal1KO show enhanced responsiveness to TGF-β1 after 48 h of treatment ($n = 3$). **d**, Immunostaining for phospho-Smad2, TGFβR2, Lef1 and Sox9 in back skin of Bmal1WT and Bmal1KO mice ($n \geq 5$). Scale bars 25 μm. **e**, Clonogenic assay of FACS-purified venus^{bright} and venus^{dim} bulge and interfollicular epidermis (IFE) keratinocytes from the back skin of P19 Per1–venus mice (7×10^3 bulge and 1×10^5 epidermal cells). Results in **a** and **c** are shown as mean ± s.e.m., $^{*}P < 0.05$ (two-tailed Student's *t*-test).

When plated at clonal density, Per1–venus^{bright} bulge stem cells and basal epidermal cells showed a higher growth potential than the corresponding venus^{dim} population, further suggesting that the clock^{high} state is more prone to become activated than the clock^{low} counterpart (Fig. 3e). Additional data confirmed this hypothesis. First, the hair follicle bulges of Bmal1KO mice, which are permanently locked in the clock^{low} state, contained fewer proliferative cells and a higher number of long-term label (BrdU)-retaining dormant stem cells (LRCs), from 10 months of age and onwards (Fig. 4a). Second, the epidermis of another model of circadian arrhythmia, Per1 and Per2 double-mutant mice (Per1/2dKO), which lacks the negative limb of the molecular clock and is therefore locked in the clock^{high} state, showed the opposite effects; that is, enhanced bulge proliferation, reduced numbers of bulge LRCs and sustained expression of epidermal clock target genes[29] (Fig. 4b and Supplementary Fig. 8). The hair follicles of Bmal1KO were less efficient in becoming active upon depilation (Supplementary Fig. 9a). Bmal1KO bulge cells were also less hyperprolifertive than wild-type bulge cells in response to treatment with the phorbol ester 12-O-tetradecanoylphorbol-13-acetate (TPA), thus delaying the entry of the hair follicles into anagen (Supplementary Fig. 9b). Lastly, epidermal stem cells purified from Bmal1KO and Per1/2dKO mice were less and more clonogenic, respectively, *in vitro* than wild-type cells (Supplementary Fig. 10a, b). Of note, deletion of *Bmal1* or *Per1/2* did not affect the proportion of bulge stem cells in adulthood compared to their controls (Supplementary Fig. 11a, b).

Loss of Bmal1 induces epidermal ageing

Reduced and enhanced proliferation, respectively, was also evident in the basal layer of the interfollicular epidermis of Bmal1KO and Per1/2dKO mice (Supplementary Fig. 12). Bmal1KO mice showed signs of inefficient epidermal self-renewal, with premature signs of ageing as early as 5 months of age, such as the accumulation of terminally differentiated cornified cells (Fig. 4c and Supplementary Fig. 9c). This was accompanied by increased expression of p16, which has been previously associated with increased epidermal ageing[30], but not p19 or apoptosis (Supplementary Fig. 13). Because bulge stem cells do not contribute to epidermal maintenance in steady-state conditions[31], we sought to understand the molecular mechanisms underlying the defects of the interfollicular epidermis of Bmal1KO mice. We performed

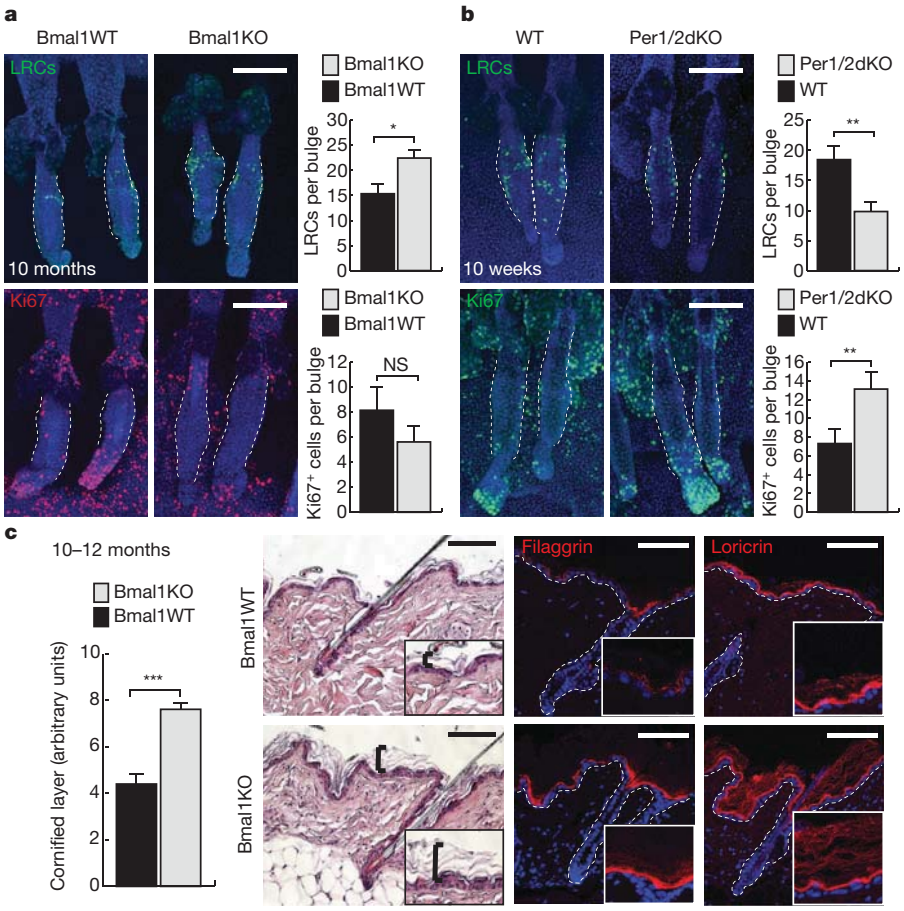

Figure 4 | Clock perturbation *in vivo* results in changes in the number of dormant bulge stem cells, and premature epidermal ageing.
a, **b**, Quantification of $BrdU^+$ LRCs and $Ki67^+$ cells in the bulge of 10-month-old Bmal1WT and Bmal1KO mice (**a**) and 10-week-old wild type (WT) and Per1/2dKO mice (**b**), showing opposite phenotypes ($n \geq 4$; 9 follicles per mouse were analysed). **c**, Histological analysis and immunostaining for filaggrin and loricrin (red) in 10–12-months-old Bmal1WT and Bmal1KO mice. Graph shows thickness quantification of the cornified layer ($n = 13$). Scale bars, 100 μm. Results are shown as mean ± s.e.m., $*P < 0.05$, $**P < 0.01$, $***P < 0.001$ (two-tailed Student's *t*-test). NS, not significant.

microarray analysis of purified basal interfollicular epidermal progenitors ($\alpha6^{bright}$/$CD34^{neg}$), from 10-month-old Bmal1KO mice and their control littermates (Supplementary Table 3). As expected, cells from Bmal1KO mice showed strong differential expression of most of the core circadian transcripts, including the microRNA miRNA-122 (ref. 32), some of which were validated independently by real-time quantitative PCR with reverse transcription (RT–qPCR) (Supplementary Fig. 14a and Supplementary Table 3). Interestingly, Gene Ontology (GO) analysis indicated that the cell cycle, energy and drug metabolism, calcium-sensing proteins, the epidermal barrier response and chromatin compaction were significantly affected upon deletion of *Bmal1* (Supplementary Fig. 14b). Intriguingly, although Bmal1KO mice showed a hyperkeratotic phenotype, the viable epidermal layers expressed lower levels of terminal differentiation markers, including *Flg*, *Lor*, *Sprr1*, *Lce* genes and *Tgm* (Supplementary Fig. 14c and Supplementary Table 3). Interestingly, Bmal1KO cells also expressed lower amounts of the miRNA-23b/-27b/-24-1 cluster, which targets TGFβR2 and Smad proteins[33] (Supplementary Fig. 14d). The reduced levels of epidermal differentiation genes probably reflects the lower efficiency of activation of basal interfollicular epidermal cells in Bmal1KO mice, suggesting that the hyperkeratotic phenotype developed as a compensatory mechanism to ensure a certain degree of epidermal barrier protection.

Loss of Bmal1 reduces skin tumorigenesis

Because perturbation of the clock machinery affects the predisposition of certain tissues to carcinogenesis[34], we next studied whether epidermal deletion of *Bmal1* had any impact on the development of cutaneous squamous tumours. To this end, we crossed Bmal1KO mice with a transgenic line expressing oncogenic Sos, an activator of Ras, under the regulation of the Krt5 promoter (K5-SOS)[35]. In an EGFR mutant-heterozygous background, K5-SOS mice spontaneously developed squamous tumours, primarily in the tail, with 100% penetrance, as previously described[35]. Bmal1KO/K5-SOS mice developed significantly fewer neoplastic lesions at early-, mid- and late-stages of carcinoma development than control mice (Fig. 5a and Supplementary Fig. 15a). The skin lesions of Bmal1KO/K5-SOS mice were more differentiated—as determined by increased expression of involucrin and loricrin—contained large cornified islands and a higher number of apoptotic areas, as compared to control tumours (Supplementary Fig. 15b). Control mice had to be killed by two months of age, a time at which no Bmal1KO mice had developed the number, or size, of tumours. The growth of cutaneous squamous tumours has been shown to depend on Wnt activity in a population of $CD34^+$ tumour-initiating cells[36]. However, we could not detect any nuclear β-catenin, either in control or in Bmal1KO neoplastic lesions, suggesting that, in our model, tumour growth did not primarily depend on misregulated Wnt signalling (Supplementary Fig. 16a, b). We did observe a significant reduction in the percentage of $\alpha6^{bright}$/$CD34^+$ tumour-initiating cells in BmalKO tumours with respect to wild-type tumours (Fig. 5b and Supplementary Fig. 17). Notably, whereas wild-type tumours expressed α6 integrin in basal and suprabasal cells, which has been previously associated with increased malignancy[37], Bmal1KO tumours only expressed it in basal

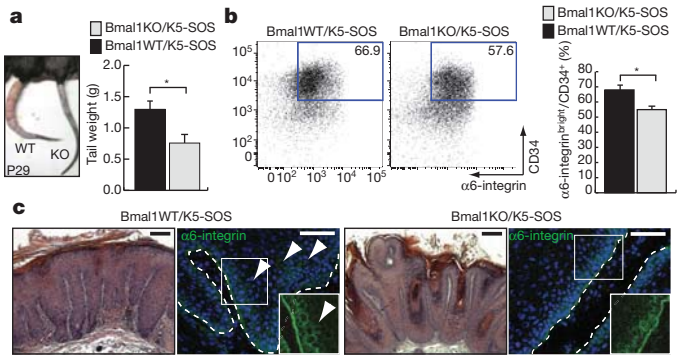

Figure 5 | Loss of Bmal1 reduces the development of squamous tumours. **a**, Quantification of tumour weight of Bmal1WT/K5-SOS and Bmal1KO/K5-SOS littermates ($n \geq 5$). **b**, FACS analysis and quantification of $\alpha6^{bright}/CD34^{+}$ tumour-initiating cells (P36 mice). Numbers represent percentage of $\alpha6^{bright}/CD34^{+}$ cells from gated epithelial cells ($n \geq 3$) **c**, Histological analysis and immunostaining for α6-integrin (arrows indicate suprabasal expression). Scale bars, 50 μm. Results in **a** and **b** are shown as mean ± s.e.m., $^{*}P < 0.05$ (two-tailed Student's *t*-test).

cells (Fig. 5c). The reduction in the percentage of tumour-initiating cells, together with the high expression of several tumour suppressors, in Bmal1KO epidermal progenitors, including the non-coding RNA H19 (top upregulated gene; Supplementary Table 3), probably contribute to the reduced burden of squamous lesions in Bmal1KO mice.

Discussion

Our results indicate that the molecular clock establishes stem cell states that are differentially predisposed to respond to activation and dormancy stimuli. The clock machinery controls the expression of essential epidermal stem cell regulators to anticipate the requirements of the tissue. In this sense, in the epidermal compartment where quiescent stem cells exist (that is, the bulge), the clock establishes a population of 'ready-to-go' cells that can rapidly and efficiently respond to activation stimuli, while simultaneously preventing all stem cells within the niche from becoming responsive. Future studies will be necessary to determine when, and how, this stem cell heterogeneity is established. On the other hand, the murine interfollicular epidermis, which primarily depends on continuously cycling basal progenitors rather than dormant stem cells[38] for its renewal, shows a much more homogenous clock activity (albeit containing approximately 5% of cells antiphasic with the majority). In this compartment the clock machinery might predominantly establish a correct timing of stem cell activation and differentiation. Conditional deletion of *Bmal1* in liver, retina and pancreas results in profound defects in tissue function[39–41], and haematopoietic stem cells show a Bmal1/Clock-dependent circadian release to the periphery[42]. Altogether, these findings indicate that the clock machinery may constitute a fine-tuning homeostatic mechanism in tissues in which dormant and active populations of stem cells coexist. Unbalancing the epidermal stem cell clock not only substantially affected long-term tissue homeostasis, but also the predisposition of the tissue to undergo neoplastic transformation. It is likely that perturbations of this clock-controlled mechanism over stem cell regulation in humans may have long-term consequences on tissue homeostasis, ageing and carcinogenesis.

METHODS SUMMARY

For the isolation of epidermal cells from back or tail skin, the skin was incubated in 0.25% trypsin for 2 h at 37 °C, or overnight at 4 °C, to separate the dermis from the epidermis. Back and tail keratinocytes were extracted as described previously[43].

For ChIP assays, cells in suspension were cross-linked for 10 min at room temperature (22–25 °C) in 1% formaldehyde. Cross-linking reactions were stopped by adding 1.25 M glycine to a final concentration of 125 mM. Cells were centrifuged at 300*g* for 10 min at 4 °C and washed in cold PBS. Cell lysis, sonification and ChIP assays were performed using the MAGnify Chromatin Immunoprecipitation System (Invitrogen).

For FACS analysis or sorting of bulge and epidermal stem cells, cell suspensions were incubated for 30 min on ice with PE-conjugated anti-α6-integrin (CD49f clone NKI-GoH3, Serotec) and biotin-conjugated anti-CD34 (clone RAM34, BD Pharmingen) antibodies followed by APC-conjugated streptavidin (BD Pharmingen) for 20 min. Dead cells were excluded by 4′,6-diamidino-2-phenylindole (DAPI) incorporation. FACS analysis and sorting were performed using LSRII FACS Analysers, FACSAriaII, FACSDiva (BD Biosciences) and Flowjo software.

For microarray analysis, total RNA was isolated from FACS-sorted cells using Trizol extraction and RNeasy Micro Kit (Qiagen). Transcriptional profiling was performed using GeneChip Mouse Gene 1.0 ST Array (Affymetrix) and functional analysis was performed using DAVID Bioinformatics Resources 6.7.

Full Methods and any associated references are available in the online version of the paper at www.nature.com/nature.

1. Fuchs, E. The tortoise and the hair: slow-cycling cells in the stem cell race. *Cell* **137,** 811–819 (2009).
2. Morris, R. J. *et al.* Capturing and profiling adult hair follicle stem cells. *Nature Biotechnol.* **22,** 411–417 (2004).
3. Tumbar, T. *et al.* Defining the epithelial stem cell niche in skin. *Science* **303,** 359–363 (2004).
4. Jaks, V. *et al.* Lgr5 marks cycling, yet long-lived, hair follicle stem cells. *Nature Genet.* **40,** 1291–1299 (2008).
5. Snippert, H. J. *et al.* Lgr6 marks stem cells in the hair follicle that generate all cell lineages of the skin. *Science* **327,** 1385–1389 (2010).
6. Jensen, K. B. *et al.* Lrig1 expression defines a distinct multipotent stem cell population in mammalian epidermis. *Cell Stem Cell* **4,** 427–439 (2009).
7. Jensen, U. B. *et al.* A distinct population of clonogenic and multipotent murine follicular keratinocytes residing in the upper isthmus. *J. Cell Sci.* **121,** 609–617 (2008).
8. Clayton, E. *et al.* A single type of progenitor cell maintains normal epidermis. *Nature* **446,** 185–189 (2007).
9. Kobielak, K., Stokes, N., de la Cruz, J., Polak, L. & Fuchs, E. Loss of a quiescent niche but not follicle stem cells in the absence of bone morphogenetic protein signaling. *Proc. Natl Acad. Sci. USA* **104,** 10063–10068 (2007).
10. Guasch, G. *et al.* Loss of TGFβ signaling destabilizes homeostasis and promotes squamous cell carcinomas in stratified epithelia. *Cancer Cell* **12,** 313–327 (2007).
11. Plikus, M. V. *et al.* Cyclic dermal BMP signalling regulates stem cell activation during hair regeneration. *Nature* **451,** 340–344 (2008).
12. Zhang, Y. V., Cheong, J., Ciapurin, N., McDermitt, D. J. & Tumbar, T. Distinct self-renewal and differentiation phases in the niche of infrequently dividing hair follicle stem cells. *Cell Stem Cell* **5,** 267–278 (2009).
13. Greco, V. *et al.* A two-step mechanism for stem cell activation during hair regeneration. *Cell Stem Cell* **4,** 155–169 (2009).
14. Enshell-Seijffers, D., Lindon, C., Kashiwagi, M. & Morgan, B. A. β-Catenin activity in the dermal papilla regulates morphogenesis and regeneration of hair. *Dev. Cell* **18,** 633–642 (2010).
15. Brownell, I., Guevara, E., Bai, C. B., Loomis, C. A. & Joyner, A. L. Nerve-derived sonic hedgehog defines a niche for hair follicle stem cells capable of becoming epidermal stem cells. *Cell Stem Cell* **8,** 552–565 (2011).
16. Flores, I., Cayuela, M. L. & Blasco, M. A. Effects of telomerase and telomere length on epidermal stem cell behavior. *Science* **309,** 1253–1256 (2005).
17. Owens, D. M. & Watt, F. M. Contribution of stem cells and differentiated cells to epidermal tumours. *Nature Rev. Cancer* **3,** 444–451 (2003).
18. Watt, F. M., Frye, M. & Benitah, S. A. MYC in mammalian epidermis: how can an oncogene stimulate differentiation? *Nature Rev. Cancer* **8,** 234–242 (2008).
19. Benitah, S. A., Frye, M., Glogauer, M. & Watt, F. M. Stem cell depletion through epidermal deletion of Rac1. *Science* **309,** 933–935 (2005).
20. Morris, R. J. A perspective on keratinocyte stem cells as targets for skin carcinogenesis. *Differentiation* **72,** 381–386 (2004).
21. Dibner, C., Schibler, U. & Albrecht, U. The mammalian circadian timing system: organization and coordination of central and peripheral clocks. *Annu. Rev. Physiol.* **72,** 517–549 (2010).
22. Cheng, H. Y. *et al.* Segregation of expression of mPeriod gene homologs in neurons and glia: possible divergent roles of mPeriod1 and mPeriod2 in the brain. *Hum. Mol. Genet.* **18,** 3110–3124 (2009).
23. Kuhlman, S. J., Quintero, J. E. & McMahon, D. G. GFP fluorescence reports period 1 circadian gene regulation in the mammalian biological clock. *Neuroreport* **11,** 1479–1482 (2000).
24. Schneider, M. R., Schmidt-Ullrich, R. & Paus, R. The hair follicle as a dynamic miniorgan. *Curr. Biol.* **19,** R132–R142 (2009).
25. Bunger, M. K. *et al. Mop3* is an essential component of the master circadian pacemaker in mammals. *Cell* **103,** 1009–1017 (2000).
26. Lin, K. K. *et al.* Circadian clock genes contribute to the regulation of hair follicle cycling. *PLoS Genet.* **5,** e1000573 (2009).

27. Kondratov, R. V., Kondratova, A. A., Gorbacheva, V. Y., Vykhovanets, O. V. & Antoch, M. P. Early aging and age-related pathologies in mice deficient in BMAL1, the core componentof the circadian clock. *Genes Dev.* **20,** 1868–1873 (2006).
28. Kameda, T. & Sugiyama, T. Application of genetically modified feeder cells for culture of keratinocytes. *Methods Mol. Biol.* **289,** 29–38 (2005).
29. Zheng, B. *et al.* Nonredundant roles of the *mPer1* and *mPer2* genes in the mammalian circadian clock. *Cell* **105,** 683–694 (2001).
30. Barradas, M. *et al.* Histone demethylase JMJD3 contributes to epigenetic control of *INK4a/ARF* by oncogenic RAS. *Genes Dev.* **23,** 1177–1182 (2009).
31. Ito, M. *et al.* Stem cells in the hair follicle bulge contribute to wound repair but not to homeostasis of the epidermis. *Nature Med.* **11,** 1351–1354 (2005).
32. Gatfield, D. *et al.* Integration of microRNA miR-122 in hepatic circadian gene expression. *Genes Dev.* **23,** 1313–1326 (2009).
33. Rogler, C. E. *et al.* MicroRNA-23b cluster microRNAs regulate transforming growth factor-β/bone morphogenetic protein signaling and liver stem cell differentiation by targeting Smads. *Hepatology* **50,** 575–584 (2009).
34. Fu, L. & Lee, C. C. The circadian clock: pacemaker and tumour suppressor. *Nature Rev. Cancer* **3,** 350–361 (2003).
35. Sibilia, M. *et al.* The EGF receptor provides an essential survival signal for SOS-dependent skin tumor development. *Cell* **102,** 211–220 (2000).
36. Malanchi, I. *et al.* Cutaneous cancer stem cell maintenance is dependent on β-catenin signalling. *Nature* **452,** 650–653 (2008).
37. Owens, D. M., Romero, M. R., Gardner, C. & Watt, F. M. Suprabasal α6β4 integrin expression in epidermis results in enhanced tumourigenesis and disruption of TGFβ signalling. *J. Cell Sci.* **116,** 3783–3791 (2003).
38. Clayton, E. *et al.* A single type of progenitor cell maintains normal epidermis. *Nature* **446,** 185–189 (2007).
39. Storch, K. F. *et al.* Intrinsic circadian clock of the mammalian retina: importance for retinal processing of visual information. *Cell* **130,** 730–741 (2007).
40. Marcheva, B. *et al.* Disruption of the clock components CLOCK and BMAL1 leads to hypoinsulinaemia and diabetes. *Nature* **466,** 627–631 (2010).
41. Lamia, K. A., Storch, K. F. & Weitz, C. J. Physiological significance of a peripheral tissue circadian clock. *Proc. Natl Acad. Sci. USA* **105,** 15172–15177 (2008).
42. Méndez-Ferrer, S., Lucas, D., Battista, M. & Frenette, P. S. Haematopoietic stem cell release is regulated by circadian oscillations. *Nature* **452,** 442–447 (2008).
43. Jensen, K. B., Driskell, R. R. & Watt, F. M. Assaying proliferation and differentiation capacity of stem cells using disaggregated adult mouse epidermis. *Nature Protocols* **5,** 898–911 (2010).

Supplementary Information is linked to the online version of the paper at www.nature.com/nature.

Acknowledgements We thank the AICR (Association for International Cancer Research), the Spanish Ministry of Health (FIS) and AGAUR (Agència de Gestió d'Ajuts Universitaris i de Recerca; Government of Cataluña) for financial support. P.J. is the recipient of an AGAUR PhD Fellowship, and G.P. of a FIS fellowship. We thank D. McMahon (Vanderbilt University) for providing us with the Per1–GFP mice; E. Wagner (CNIO) for the K5-SOS mice; B. Kübler, the FACS and Genomics units of the IRB (Institute de Recerca Biomedica), the CRG (Center for Genomic Regulation) core facilities and the Animal Unit (Juan Martin Caballero) for technical support.

Author Contributions P.J. performed the experiments, and P.J. and S.A.B. analysed the results and wrote the manuscript. G.P. performed the analysis of K5-SOS mice, and A.M. and E.B. assisted P.J. in the initial FACS sorts. L.D.C. helped us with the initial ChIP experiments. K.O. provided the Per1–venus mice. J.R. and U.A. provided the Per1/Per2dKO mice.

Author Information Microarray data can be retrieved from the Gene Expression Omnibus under accession number GSE27079. Reprints and permissions information is available at www.nature.com/reprints. The authors declare no competing financial interests. Readers are welcome to comment on the online version of this article at www.nature.com/nature. Correspondence and requests for materials should be addressed to S.A.B. (salvador.aznar-benitah@crg.es).

METHODS

Animals. Bmal1$^{LoxP/LoxP}$ and K14Cre mice purchased from The Jackson Laboratory were crossed with each other to obtain K14Cre/Bmal1$^{wt/wt}$ (Bmal1WT) and K14Cre/Bmal1$^{LoxP/LoxP}$ (Bmal1KO), and with K5-SOS mice to generate K14Cre/Bmal1$^{wt/wt}$/K5-SOS (Bmal1WT/K5SOS) and K14Cre/Bmal1$^{LoxP/LoxP}$/K5-SOS (Bmal1KO/K5SOS) littermate controls[35]. Per1–GFP and Per1–venus mice have been described previously[22,23]. K14Cre/Bmal1$^{wt/wt}$ Per1–venus and K14Cre/Bmal1$^{LoxP/LoxP}$ Per1–venus mice were generated by crossing K14Cre/Bmal1$^{wt/wt}$ and K14Cre/Bmal1$^{LoxP/LoxP}$ animals with Per1–venus mice, respectively. *Per1* and *Per2* double-mutant mice (Per1/2dKO) have been described previously, and were compared to age and sex-matched control animals to avoid differences in hair cycle behaviour between males and females[29]. Mice were housed in an AAALAC-I approved animal unit under 12 h light/12 h dark or 12 h dark/12 h dark cycles, and SPF conditions, and all procedures were approved by the CEEA (Ethical Committee for Animal Experimentation) of the Government of Catalonia. For experiments in constant darkness, light was turned off at Zeitgeber time (ZT)12 and animals were housed in 12 h dark/12 h dark conditions for 5 days. For 5-bromo-2-deoxyuridine (BrdU)-labelling experiments, 100 μg g^{-1} BrdU (Invitrogen) was injected intraperitoneally into the mice and chased for 10 weeks or up to 10 months, as indicated. To activate epidermal proliferation, back skin or tail skin of 10-week-old Bmal1WT and Bmal1KO mice was treated three times with 20 nM TPA (Sigma-Aldrich) during one week. For depilation experiments, dorsal skin of 15-month-old Bmal1WT and Bmal1KO mice in telogen phase was depilated with cold wax strips (Taky).

Primary mouse keratinocyte cultures. Primary mouse keratinocytes from newborn mice or tail skin of adult mice were isolated as described previously[43,44]. Cells were plated in EMEM (Lonza) containing 4% chelated FBS, 1% penicillin/streptomycin and 20 nM calcium for 24 h; medium was then changed to growth medium (EMEM with 4% chelated FBS, 1% penicillin/streptomycin, EGF (10 ng ml^{-1}) and 50 nM calcium). For the time-course experiments of keratinocytes isolated from Bmal1WT or Bmal1KO mice, cells were synchronized by a serum shock with growth medium, containing 50% chelated FBS, for 2 h[45]. For TGF-β treatments, keratinocytes were cultured in the presence of TGF-β1 (2 ng ml^{-1}; PreproTech) for 48 h. For clonogenic assays, the indicated number of FACS-sorted keratinocytes were plated in E-medium on mitomycin (Sigma-Aldrich)-treated J2 3T3 feeder cells[46]. Keratinocytes were grown at 37 °C with 5% CO_2.

Whole-mount immunofluorescence. Preparation of tail skin and whole-mount stainings were performed as previously described[47]. Primary and secondary antibodies were incubated overnight and used at the following concentrations: 1:1,000 for anti-GFP (A11122, Invitrogen); 1:250 for anti-BrdU (Serotec) and anti-Ki67 (ab15580, Abcam; clone B56, BD Pharmingen); and 1:500 for anti-rabbit and anti-rat conjugated to AlexaFluor488 or AlexaFluor594 (Molecular Probes). Nuclei were stained with DAPI (1:5000; Roche), and epidermal sheets were mounted in Mowiol. Pictures were acquired with a Leica TCS SP5 confocal microscope.

Immunohistochemistry. Back skin and tail skin were either embedded in OCT, or fixed in 4% NBF (Sigma-Aldrich) at 4 °C overnight or 2 h at room temperature (22–25 °C) and then embedded in paraffin or OCT. Deparaffinized sections were boiled for 10 min in 0.01 M citric acid for antigen retrieval. For permeabilization, 8-μm slices of either cryosections, or sections that had been deparaffinized or antigen retrieved were permeabilized for 25 min in 0.25% Triton X-100/PBS and blocked for 90 min in 0.25% gelatin/PBS. Primary antibodies were incubated overnight at 4 °C, and secondary antibodies were incubated for 2 h at room temperature in 0.25% gelatin/PBS. Nuclei were stained with DAPI (1:5,000, Roche), and the slides were mounted in Mowiol. Primary antibodies were used at the following dilutions: 1:50 for anti-p19 (M-167, Santa Cruz), anti-p16 (M-156, Santa Cruz); 1:100 for anti-Sox9 (H-90, Santa Cruz); 1:200 for anti-α6-integrin (CD49f clone NKI-GoH3, Serotec), anti-keratin 14 (ab7800, Abcam); 1:250 for anti-Ki67 (ab15580, Abcam); 1:500 for anti-keratin 5 (ab24647, Abcam); and 1:1,000 for anti-GFP (ab290, Abcam; A11122, Invitrogen), anti-involucrin (PRB-140C, Covance), anti-filaggrin (ab24584, Abcam), anti-loricrin (PRB-145P, Covance), anti-phospho-Smad2 (#3101, Cell Signaling), anti-Lef1 (clone C12A5, Cell Signaling). Secondary antibodies were used at dilutions of 1:500: anti-rabbit, anti-mouse, or anti-rat, conjugated to AlexaFluor488 or AlexaFluor594 (Molecular Probes), or anti-rabbit biotin (GE Healthcare), followed by an incubation with ABC Kit (Vector Laboratories) and FAST 3,3 Diaminobenzidine tablets (Sigma-Aldrich). For apoptosis measurements, tail skin was stained with the DeadEnd Fluorometric TUNEL System (Promega). Staining with haematoxilin or eosin was done according to a standard protocol. Pictures were acquired with a Leica DMI 6000B or a Leica TCS SP5 confocal microscope.

Time-lapse microscopy and quantification. For time-lapse confocal imaging, back skin of Per1–venus mice was fixed with 0.5% agarose in an imaging dish (Ibidi) and over-layered with E-medium. Images were taken every 15 min for a period of 48 h using a Leica TCS SP5 confocal microscope equipped with a tempered chamber of 37 °C and 5% CO_2. Mean fluorescence intensity of individual GFP-positive nuclei was quantified using ImageJ software.

FACS. Epidermal cells from back skin of Per1–venus, Bmal1WT and Bmal1KO mice, or tail skin of Bmal1WT/K5-SOS and Bmal1KO/K5-SOS mice, were isolated as described previously[43]. Per1–venus mice were killed between ZT10–ZT12 or as specified in the figure legends. Cell suspensions were incubated for 30 min on ice with the following antibodies at the given dilutions: 1:100 for biotin- or APC-conjugated anti-CD34 (clone RAM34, BD Pharmingen), PE-conjugated anti-CD31 (clone MEC13.3, eBioscience), PE-conjugated anti-CD45 (clone 30F11, eBioscience), PE-conjugated anti-CD140a (clone APA5, BD Pharmingen) and APC-Cy7-conjugated anti-epcam (clone G8.8, Biolegend); 1:200 for PE- or FITC-conjugated anti-α6-integrin (CD49f clone NKI-GoH3, Serotec); and 1:500 for APC-conjugated streptavidin (BD Pharmingen). DAPI staining was used to rule out that dead cells were present. FACS was performed using FACSAriaII and FACSDiva software (BD Biosciences). Sorted cells were collected in E-medium, either plated in culture or re-suspended in Trizol (Invitrogen), and subjected further to RNA isolation. FACS analysis was performed using LSRII FACS Analysers (BD Biosciences) and Flowjo software.

Arrays. Total RNA was isolated from FACS-sorted cells in Trizol by chloroform extraction, followed by the RNA clean-up protocol of RNeasy Micro or Mini Kit (Qiagen). Transcriptional profiling was performed using GeneChip Mouse Gene 1.0 ST Array (Affymetrix). Arrays of venus^{bright} and venus^{dim} bulge cells of P19 Per1–venus mice were performed as triplicates from a pool of $n = 64$ mice. Arrays of epidermal cells from 10-months-old Bmal1WT and Bmal1KO mice were performed as triplicates using three independent mice in each group. Functional analysis of microarray data was performed using DAVID Bioinformatics Resources 6.7.

RT–qPCR. Total RNA from cultured or FACS-sorted cells was purified as described above, or using either the RNeasy Micro and Mini Kit (Qiagen) or miRVana miRNA isolation Kit (Ambion). Equal amounts of RNA were reverse-transcribed using Superscript III (Invitrogen). RT–qPCR was performed with SYBR Green Master Mix (Roche) and gene-specific primers (as given in Supplementary Table 4)[48] using a Light Cycler 480 Instrument (Roche). Relative levels of expression were determined by normalization to pumilio 1 (Pum1), using the $\Delta\Delta C_t$ method.

ChIP. For ChIP assays from intact epidermis, mice were killed at ZT2, or for time-course analysis every 3 h during a period of 24 h, and tails were incubated in 0.25% trypsin for 2 h at 37 °C to separate the dermis from the epidermis. Tail keratinocytes were extracted as described[43]. Cells in suspension or FACS-purified cells (2×10^5) were cross-linked for 10 min at room temperature in 1% formaldehyde. Cross-linking reactions were stopped by adding 1.25 M glycine to a final concentration of 125 mM. Cells were centrifuged at 300*g* for 10 min at 4 °C and washed in cold PBS. Cell lysis, sonification and ChIP assays were performed using the MAGnify Chromatin Immunoprecipitation System (Invitrogen). For each immunoprecipitation, 2×10^5–10^6 cells were incubated with 2 μl of anti-Bmal1 or anti-Clock antibody (provided by J. Ripperger, University of Fribourg)[49], or 2 μl of rabbit IgG control antibody (Invitrogen). RT–qPCR was performed as described above using gene-specific primers (Supplementary Table 5).

Genotyping and western blots. Genomic DNA of primary mouse keratinocytes from Bmal1WT and Bmal1KO mice was isolated using a standard protocol. Multiplex PCR was performed as previously described to determine recombination efficiency[39]. Protein extracts from newborn keratinocytes or from tail epidermis were analysed by SDS–PAGE and western blotting for Bmal1 (ref. 49), anti-phospho-Smad2 (1:1,000, #3101, Cell Signaling), anti-Lef1 (1:1,000, clone C12A5, Cell Signaling), anti-Sox9 (1:400, H-90, Santa Cruz) and anti-tubulin (1:5,000, Sigma Aldrich)

Luciferase assay. Primary mouse keratinocytes were transiently transfected with either FOP-Flash or TOP-Flash and pCMV-Renilla plasmids using FuGENE6 (Roche) according to the manufacturer's instructions. The TOP-Flash construct reports Wnt activity by driving the expression of Luciferase under the regulation of TCF-Lef binding sites. FOP-Flash contains the same binding sites mutated so that they are no longer responsive to TCF/Lef. Cells were treated in the absence or presence of 1 μM BIO (Calbiochem) at 48 h post-transfection for a period of 24 h. Luciferase activity was measured in a Centro LB 960 luminometer (Berthold Technologies) using Dual-Luciferase Reporter Assay System (Promega).

Promoter analysis. Gene promoter analysis for potential Bmal1/Clock-binding sites (in general, from −5,000 to +1,000 bases from the transcriptional start site) were analysed using Genomatix Software.

Statistics. Results are presented as mean ± s.e.m. Statistical significance was determined by two-tailed Student's *t*-test, one-way ANOVA, two-way ANOVA

with Bonferroni post-test, or Cosinor analysis. A P value of $P \leq 0.05$ was considered to be statistically significant.

44. Litchi, U., Anders, J. & Yuspa, S. Isolation and short-term culture of primary keratinocytes, hair follicle populations and dermal cells from newborn mice and keratinocytes from adult mice for *in vitro* analysis and for grafting to immunodeficient mice. *Nature Protocols* **5,** 799–810 (2008).
45. Balsalobre, A., Damiola, F. & Schibler, U. A serum shock induces circadian gene expression in mammalian tissue culture cells. *Cell* **93,** 929–937 (1998).
46. Nowak, J. A. & Fuchs, E. Isolation and culture of epithelial stem cells. *Methods Mol. Biol.* **482,** 215–232 (2009).
47. Braun, K. M. *et al.* Manipulation of stem cell proliferation and lineage commitment: visualization of label-retaining cells in wholemounts of mouse epidermis. *Development* **130,** 5241–5255 (2003).
48. Sun, F. *et al.* Characterization of function and regulation of miR-24-1 and miR-31. *Biochem. Biophys. Res. Commun.* **380,** 660–665 (2009).
49. Ripperger, J. & Schibler, U. Rhythmic CLOCK-BMAL1 binding to multiple E-box motifs drives circadian *Dbp* transcription and chromatin transitions. *Nature Genet.* **38,** 369–374 (2006).